ELSEVIER

Journal of Hazardous Materials A89 (2002) 109–125

Journal of Hazardous Materials

www.elsevier.com/locate/jhazmat

Modelling top venting vessels undergoing level swell

Peter Cumber*

Department of Mechanical and Chemical Engineering, Heriot Watt University, Edinburgh EH14 4AS, UK

Received 8 May 2001; received in revised form 29 August 2001; accepted 29 August 2001

Abstract

The storage and processing of fluids in a two-phase state at pressure requires the consequences of a failure of the vessel wall or a pipe break due to corrosion or third party interference, be considered as part of a safety analysis. The present paper describes a mathematical model for predicting outflow rates from top venting high-pressure vessels undergoing level swell. A key aspect of the models development is there are no free parameters that require adjustment to predict the correct outflow from a top venting vessel. The mathematical model is validated by comparing predicted flow parameters such as vessel pressure and mass flow rate with measurements and existing mathematical models. The new model agrees more closely with the experimental measurements than previous approaches over the range of experimental conditions considered.

Keywords: Level swell; Vessel outflow; Consequence assessment

1. Introduction

The storage and processing of fluids in a two-phase state at pressure requires the consequences of a failure of the vessel wall or a pipe break due to corrosion or third party interference be considered, as part of a safety analysis. The present paper describes a mathematical model for predicting outflow rates from top venting high-pressure vessels undergoing level swell. This scenario is of interest in a number of different industries, for example the nuclear industry where the loss of coolant from the reactor must be considered, or the assessment of gas, oil and condensate storage and processing plant. In this context, an outflow model provides source conditions for consequence models of fire and dispersion

* Tel.: +44-131-451-3532.
E-mail address: p.s.cumber@hw.ac.uk (P. Cumber).

PII: S0304-3894(01)00334-X

Nomenclature

A_{vent}	vent area
$A_{ves,cros}$	cross-sectional area of the vessel
C_0	radial distribution parameter
C_0^{open}	radial distribution parameter for an open system
E	internal energy
g	gravitational constant
H	enthalpy
j_L	liquid phase superficial velocity
j_G	gas phase superficial velocity
m_T	mass in vessel
$\dot{m}_{vent}$	mass flow rate
$\dot{m}_{vent,G}$	mass flow rate of a gas phase release
N_ν	parameter in the bubble rise velocity correlation (l)
t	time co-ordinate
U_{bub}	bubble rise velocity
U_G	area averaged gas phase velocity
U_L	area averaged liquid phase velocity
V_G	volume of gas
V_L	volume of liquid
x_q	stagnation vapour quality

Greek letters

η	closed system multiplier function for the radial distribution parameter
ν_f	vessel void fraction
ν_L	kinematic viscosity of the liquid phase
ρ_G	gas phase density
ρ_L	liquid phase density
σ	surface tension
Ω	ratio of the vent area to the vessel cross-sectional area
ψ	dimensionless gas phase superficial velocity
ψ_{max}	maximum dimensionless gas phase superficial velocity

Subscripts

α	a gas, liquid or two-phase quantity
G	a gas phase quantity
L	a liquid phase quantity

Superscripts

DIERS	quantity used in the DIERS methodology
open	an open system parameter

as well as providing a tool for estimating the time a vessel takes to blowdown following emergency depressurisation.

A model for the prediction of outflow from a vessel where level swell effects are not important has been described previously [1]. The outflow models extension to include level swell is described and evaluated below.

When top venting occurs from a vessel in a two-phase state, there is initially all vapour venting and the pressure drops. As the pressure falls, the liquid becomes increasingly superheated and bubbles form. This may cause level swell with the two-phase fluid vapour interface rising up the vessel. If the interface approaches within a certain critical distance of the vent, entrainment of liquid droplets into the vent may occur. If the interface reaches the vent, two-phase venting is likely, with the vessel pressure increasing. The rise in pressure occurs as the volumetric rate of flow through the vent reduces when two-phase venting occurs, whereas the vapour volume production from the superheated liquid is initially maintained. The pressure reaches a maximum and ultimately the interface falls below the vent entrance and all vapour venting prevails again. The process is illustrated schematically in Fig. 1. The time-scale for the process depends on the vessel and vent size. For a laboratory size vessel with a vessel height of less than 1 m the time from the onset of the depressurisation to the pressure maximum is typically of the order of several seconds.

The model considered in this paper, similar to other models [2], assumes two-phase venting occurs instantaneously, ignoring the initial rapid decrease and recovery in vessel pressure, as it occurs over a short time interval and adds little to the consequence assessment. However, other studies have investigated the initial transient phase [3,4] where bubble

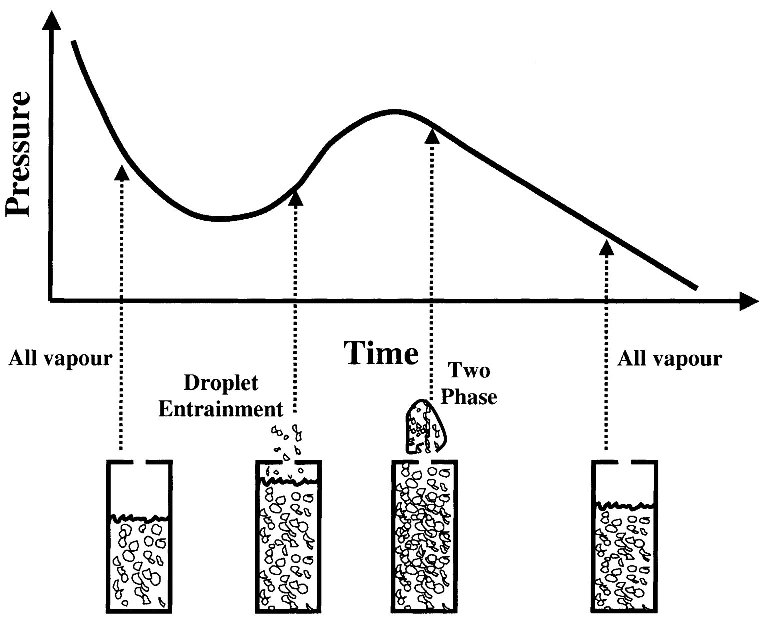

Fig. 1. Typical depressurisation behaviour of a top venting vessel undergoing level swell.

growth, level swell and droplet entrainment are considered. The models developed in [3,4] are however not at a stage of development for general application as they include a number of parameters that must be estimated, such as the average bubble diameter.

There are three possible ways in which the two-phase fluid–vapour interface may behave, governing the quality of the fluid at the vent; complete vapour–liquid disengagement, partial vapour–liquid disengagement and no vapour–liquid disengagement. When complete vapour–liquid disengagement occurs the vapour and liquid phases separate completely at a plane below the vent, giving a release of vapour. Partial vapour–liquid disengagement gives a partial separation of the vapour and liquid at the interface so that the vapour quality entering the vent is higher than that of the bulk fluid. The final possibility of no vapour–liquid disengagement, the vapour and liquid phases are uniformly mixed and there is no separation at the interface. The quality of the fluid entering the vent is the same as the bulk fluid in the vessel. This is often known as the homogeneous frothing or foaming condition.

The factors influencing the behaviour of the interface are; the initial liquid height in the vessel, the fluid composition and properties, vessel pressure, vapour production rate, vessel flow regime and vent size.

A number of models exist for predicting the depressurisation of a top venting two-phase vessel developed to address the needs of the nuclear industry and the chemical processing industry. Skouloudis [2] described a number of models, comparing their basis and accuracy for a range of vessel and vent geometries and working fluids. For example SAFIRE contains a vessel depressurisation model developed for the DIERS group, a collaborative group of companies with an interest in assessing overpressure due to runaway reactions in batch processes [2]. SAFIRE has a range of vent models available requiring a user to be well versed in outflow modelling, and any predicted outflow is likely to be dependant on the user of the model. Another difficulty with SAFIRE is that its numerical implementation is not robust, often failing. The numerical problems in SAFIRE have largely been overcome in an updated model called SUPERCHEMS. Another model discussed in [2] is RELAP, a vessel depressurisation model developed for analysing the loss of coolant in a nuclear reactor. The working fluid in RELAP is restricted to water although JRC ISPRA have extended the model to include other fluids.

The model described below differs from SAFIRE and RELAP as it has been developed with a view to calculating source conditions for other consequence models, primarily for the safety assessment of hydrocarbon storage and processing systems. The model user is not expected to have an in-depth knowledge of how to model outflow from high-pressure multiphase vessels. All issues relating to outflow modelling such as which type of vent model to use, for a given set of vessel operating conditions and optimal values for parameters in the level swell model are all part of the model rather than input by the user. This is possible as a simple theory extending the work of Kataoka and Ishii [5], for bubble columns to vessels has been developed and is described below.

2. Description of the model

The transient behaviour of a vessel's contents when depressurising, treating the vessel as a single control volume is described by equations for the conservation of mass and energy:

$$\frac{dm_T}{dt} = -\dot{m}_{vent}$$

$$\frac{d(mE)_T}{dt} = -\dot{m}_{vent} H_\alpha$$

$$m_T = \rho_G V_G + \rho_L V_L$$

$$(mE)_T = \rho_G V_G E_G + \rho_L V_L E_L$$

where m_T denotes the mass in the vessel, E is the internal energy, and ρ and V are the density and volume of a given phase. The subscripts G and L refer to gas and liquid phase quantities, respectively. The subscript α refers to the phase of the venting fluid, which can be either in a gas, liquid or two-phase state. No heat transfer between the vessel surroundings and its contents via the vessel wall is considered as its influence on the mass flow rate is small in the initial stages of discharge, when the mass flow rate is at its largest.

The system of equations is closed by assuming thermodynamic equilibrium between the two phases. This assumption is not always valid, particularly when rapid depressurisation occurs, but Cumber [1] showed that apart from level swell, non-equilibrium effects have a small influence on the predicted mass flow rate.

The liquid and gas phase density are calculated using the COSTALD method [6], and the Peng–Robinson equation of state (EOS) [6], respectively. A number of different equations of state were evaluated as part of the outflow models development, such as the Soave version of the Redlich Kwong EOS [6] and a generalisation of the Soave version of the Redlich Kwong EOS for polar fluids [7], with little sensitivity of the mass flow rate to the EOS exhibited.

3. Vent models

Considering the mass loss term (m_{vent}) a number of possible vent types and phase of release are possible. Flow through an orifice or pipe are considered together with gas or two-phase releases. Liquid outflow was considered in a previous paper [1]. For a gas phase release through an orifice the mass flow rate is calculated using the isentropic ideal nozzle flow equations [8], with the modification that the static density is calculated by the Peng–Robinson EOS. The use of a cubic equation of state to calculate the gas phase density rather than the ideal equation of state, a common approach, significantly improves the vent models accuracy for a modest increase in computer run-time [1]. In the vent models, a discharge coefficient is included to account for non-ideal effects. The value of the discharge coefficient used is 0.8 for gas or two-phase flow, typical of a sharp edged sudden contraction.

Gas outflow from a pipe is calculated by assuming the flow of gas from the vessel to the pipe entrance as isentropic and the flow of gas along the pipe to be isenthalpic with frictional effects included. The fanning friction factor is a function of wall roughness and Reynolds number [9].

To calculate the mass flow rate for a two-phase fluid through an orifice, the homogeneous equilibrium model is used. The two-phase mixture is treated as a single fluid with the two phases taken to be in equilibrium with equal velocities and temperatures. Two-phase flow through a pipe is calculated by solving an equation for the conservation of momentum under the homogeneous equilibrium assumption for two-phase flow [9].

4. Level swell model

The final aspect of predicting vessel depressurisation of a two-phase vessel is the level swell model. The level swell model does not take into account the time taken for the swell height to reach its maximum extent and assumes two-phase venting occurs instantaneously. This gives conservative predictions of outflow early in the vessel depressurisation event. The basis for estimating level swell is a drift flux model [10]. The level swell model will be discussed for a churn turbulent flow regime, but is also applicable with minor modifications to the bubbly flow regime. The level swell model described below follows the DIERS methodology [9], with a number of improvements developed recently.

The superficial velocity of the liquid and gas phases are

$$j_{\mathrm{L}} = U_{\mathrm{L}}(1-\nu_{\mathrm{f}}), \qquad j_{\mathrm{G}} = U_{\mathrm{G}}\nu_{\mathrm{f}}$$

where U_{L} and U_{G} are the area averaged liquid and gas phase velocities in the vessel and ν_{f} is the vessel void fraction. Using the drift flux model, the superficial velocities of the liquid and gas phases can be related to the bubble rise velocity:

$$\nu_{\mathrm{f}} U_{\mathrm{bub}} = (1 - C_0\nu_{\mathrm{f}})\, j_{\mathrm{G}} - C_0\nu_{\mathrm{f}}\, j_{\mathrm{L}}$$

where U_{bub} is the bubble rise velocity and C_0 is a radial distribution parameter:

$$C_0 = \frac{\langle \nu_{\mathrm{f}}(j_{\mathrm{L}} + j_{\mathrm{G}})\rangle}{\langle \nu_{\mathrm{f}}\rangle\langle j_{\mathrm{L}} + j_{\mathrm{G}}\rangle}$$

where the angled brackets indicate quantities averaged over the cross-sectional area of the vessel. The radial distribution parameter is introduced into the analysis to take into account the non-uniform distribution of bubble formation in the vessel liquid space. The parameter value $C_0 = 1$ defines a uniform void distribution. The bubble rise velocity correlation implemented is

$$U_{\mathrm{bub}} = \begin{cases} 0.03\left[\dfrac{\sigma g(\rho_{\mathrm{L}} - \rho_{\mathrm{G}})}{\rho_{\mathrm{L}}^2}\right]^{0.25}\left[\dfrac{\rho_{\mathrm{G}}}{\rho_{\mathrm{L}}}\right]^{-0.157} N_\nu^{-0.562}, & N_\nu \le 0.00225 \\[2ex] 0.92\left[\dfrac{\sigma g(\rho_{\mathrm{L}} - \rho_{\mathrm{G}})}{\rho_{\mathrm{L}}^2}\right]^{0.25}\left[\dfrac{\rho_{\mathrm{G}}}{\rho_{\mathrm{L}}}\right]^{-0.157}, & 0.00225 < N_\nu \le 0.1 \end{cases} \tag{1}$$

$$N_\nu = \frac{\nu_{\mathrm{L}}\rho_{\mathrm{L}}}{\sqrt{\rho_{\mathrm{L}}\sigma\sqrt{\sigma/g(\rho_{\mathrm{L}} - \rho_{\mathrm{G}})}}}$$

where σ is the surface tension and ν_L is the liquid phase kinematic viscosity. Wehmeir et al. [11] showed that this formulation was a significant improvement over the equation:

$$U_{bub}^{DIERS} = 1.53\left[\frac{\sigma g(\rho_L - \rho_G)}{\rho_L^2}\right]^{0.25} \tag{2}$$

for correlating the gas phase mass flux in bubble columns. The DIERS superscript in Eq. (2) is introduced to indicate that this is the bubble rise velocity implemented in the DIERS methodology [9]. Continuity of the flow at the vent during two-phase venting in a vessel and the drift flux model gives the equation:

$$j_G = \frac{U_{bub}\nu_f}{1 - C_0\nu_f[1 + (1 - x_q/x_q)(\rho_G/\rho_L)]} \tag{3}$$

where x_q is the stagnation vapour quality. The vapour mass flow rate entering the vent also satisfies the equation:

$$j_G = \frac{x_q \dot{m}_{vent}}{\rho_G A_{ves,cros}} \tag{4}$$

where $A_{ves,cros}$ is the cross-sectional area of the vessel. Combining Eq. (3) with Eq. (4) gives an equation coupling the vessel and vent conditions. The coupling equation can be solved iteratively to give the stagnation quality at the vent entrance. The above analysis is for a vessel with a constant cross-section. Recently, Sheppard [12], has extended the analysis to level swell in spheres and horizontal cylinders, although the correlations derived are similar to those found in [9] for a vertical cylinder.

The next modelling issue addressed is the vessel and vent conditions for which two-phase venting occurs. It is convenient to define the dimensionless superficial gas velocity:

$$\psi = \frac{j_G}{U_{bub}}$$

In the DIERS methodology, for churn turbulent flow, the boundary between gas phase and two-phase venting is given by the correlation:

$$\psi^{DIERS}(\nu_f) = \frac{2\nu_f}{1 - C_0\nu_f} \tag{5}$$

Sheppard and Morris [13], derived an exact form for the relationship between the dimensionless superficial gas velocity and vessel void fraction in the implicit form:

$$\nu_f = 1 + \frac{\psi(1 - C_0)^2}{\ln[1 + (C_0 - 1)\psi] - C_0(C_0 - 1)\psi} \tag{6}$$

by formulating and solving an energy balance for a differential slice in a vessel. Eq. (6) is implemented in the level swell model, rather than the DIERS correlation (5).

The maximum dimensionless superficial gas velocity (ψ_{max}) occurs for all gas venting, and the predicted vent phase is determined by the condition:

$$\psi(\nu_f) < \psi_{max} \Rightarrow \text{two phase venting}, \qquad \psi(\nu_f) \geq \psi_{max} \Rightarrow \text{gas phase venting}$$

In the DIERS methodology, the maximum dimensionless superficial gas velocity also gives an indication of the most likely flow regime:

$$\psi_{\mathrm{max}} \leq 0.2 \text{ bubbly flow regime}, \qquad 0.2 < \psi_{\mathrm{max}} \leq 20 \text{ churn turbulent flow regime}, \\ 20 < \psi_{\mathrm{max}} \text{ homogeneous flow regime}$$

However, it should be noted that this is not appropriate where small concentrations of foaming agents have been introduced to the vessel.

The above analysis is a brief description of the level swell model. More details can be found in [8–12].

To close the model the radial distribution parameter C_0 remains to be specified. In some previous vessel depressurisation studies C_0 was treated as a free parameter adjusted for each scenario considered to gain agreement with measured flow parameters, but with little or no generality [7]. Kataoka and Ishii [5], proposed the functional form:

$$C_0^{\mathrm{open}} = 1.2 - 0.2\sqrt{\frac{\rho_{\mathrm{G}}}{\rho_{\mathrm{L}}}} \tag{7}$$

for open round bubble columns, however this tends to under predict the radial distribution parameter for gas phase to liquid phase density ratios of less than 0.01. In this paper, the following power law correlation is proposed:

$$C_0^{\mathrm{open}} = \left(\frac{\rho_{\mathrm{G}}}{\rho_{\mathrm{L}}}\right)^{-0.05} \tag{8}$$

Fig. 2 shows the measured radial distribution parameter for open round bubble columns. Kataoka and Ishii [5] and the proposed power law fit (8), are also shown. The two correlations are similar for density ratios above 0.1. For density ratios below 0.1 the power law correlation differs from Kataoka and Ishii's correlation and is a better fit to the experimental data.

To derive the radial distribution parameter for a top venting vessel undergoing level swell, an extension of the open system correlation is proposed. A vessel differs from an open system when the liquid level is sufficiently high as the pressure field is distorted by the outflow at the vent, which in turn influences the bubble distribution. The radial distribution parameter for a closed system is postulated to have the form:

$$C_0 = C_0^{\mathrm{open}} \eta(\nu_{\mathrm{f}}, \Omega), \qquad \Omega = \frac{A_{\mathrm{vent}}}{A_{\mathrm{ves,cros}}} \tag{9}$$

where η is a closed system multiplier function. The functional form for η has the theoretical limits:

$$\nu_{\mathrm{f}} \to 1 \Rightarrow \eta \to 1, \qquad \Omega \to 1 \Rightarrow \eta \to 1$$

For top venting two-phase vessels:

$$\Omega \ll 1$$

Therefore, as there is limited data available it is assumed, that the Ω dependency can be ignored. Using experimental data for top venting two-phase vessels taken from the

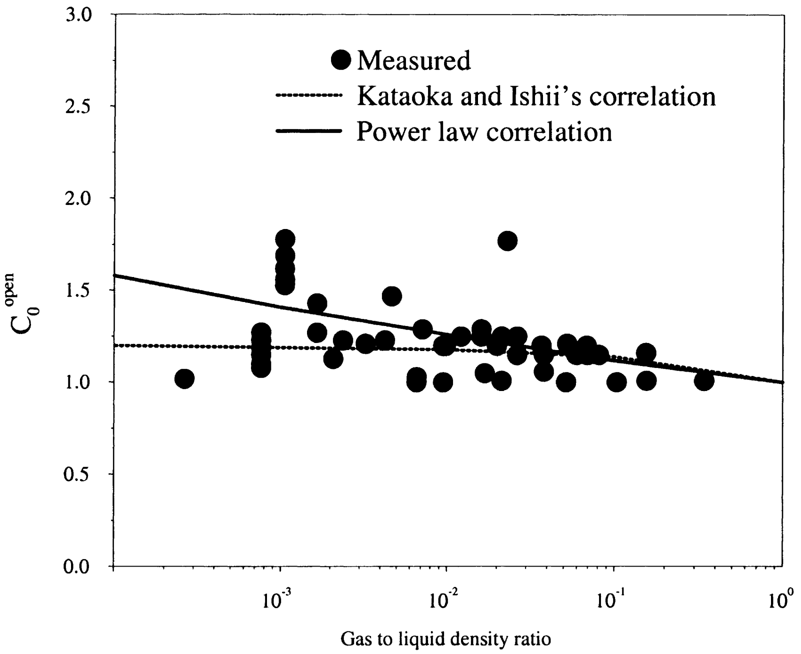

Fig. 2. Radial distribution parameter for round bubble columns.

open literature [2,9,11] to calibrate Eq. (9), an expression for the closed system multiplier function, η can be derived. The simplest functional form for the closed system multiplier function is

$$\eta = \max\{1, A - B\nu_f\} \tag{10}$$

where it is assumed that for

$$\frac{A-1}{B} \leq \nu_f$$

the top venting vessel with respect to level swell behaves like an open system. Calibrating the above functional form (10), with the open literature data gives the expression:

$$\eta = \max\{1, 2.6 - 8.4\nu_f\} \tag{11}$$

Fig. 3 shows the goodness of fit for the function, η with the experimental data. There is some scatter in the experimental data, but no more than that used in the open system bubble column data. In Fig. 3 some of the data points violate the theoretical lower bound of unity for the closed system multiplier function, and these should be viewed as a comment on the goodness of fit of the open system correlation. The points labelled as "measured" in Fig. 3 represent the best fit of the outflow model to the measured data achieved by adjusting the radial distribution parameter. Implicit in the scatter in the data are the experimental errors, but more significantly any shortcomings of the two-phase vent model. This issue is

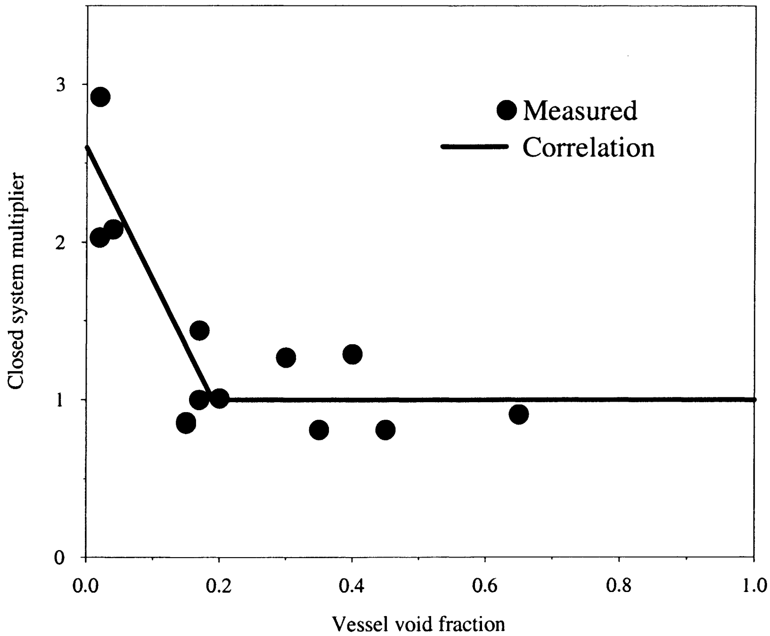

Fig. 3. Closed system multiplier function for the radial distribution parameter, Eq. (11).

considered further below. The experimental data used to calibrate η has a range of initial pressures up to 11 bar, vessels with a maximum volume of 2300 l and a range of fill levels, from 70 to 98% of the vessel volume.

5. Model evaluation

Implicit in the calibration of the closed system multiplier function, η is the two-phase vent model implemented. The gas phase vent model implemented is well accepted, whereas for two-phase venting the situation is less clear, with many different two-phase venting models in the open literature. Fig. 4 shows some of the validation study used to demonstrate that the homogeneous equilibrium model is sufficiently accurate for hydrocarbon systems. The sources for the measured mass flow rates are [14,15]. The flow conditions range from liquefied natural gas to mixtures of hydrocarbons including propane, butane and heptane, and stagnation pressures of up to 100 bar.

It should be noted that the majority of the data in Fig. 4 is for mass flow rates through orifice plates. The good agreement between the homogeneous equilibrium model and measured mass flow rates for the flow of hydrocarbon mixtures through orifice plates, verified independently by Hewit et al. [14] is unexpected based on studies with other fluids [16]. Danby [16], showed that for water–air systems and steam–water systems, the homogeneous equilibrium model was accurate for vents with lengths of 150 mm or more, but for shorter

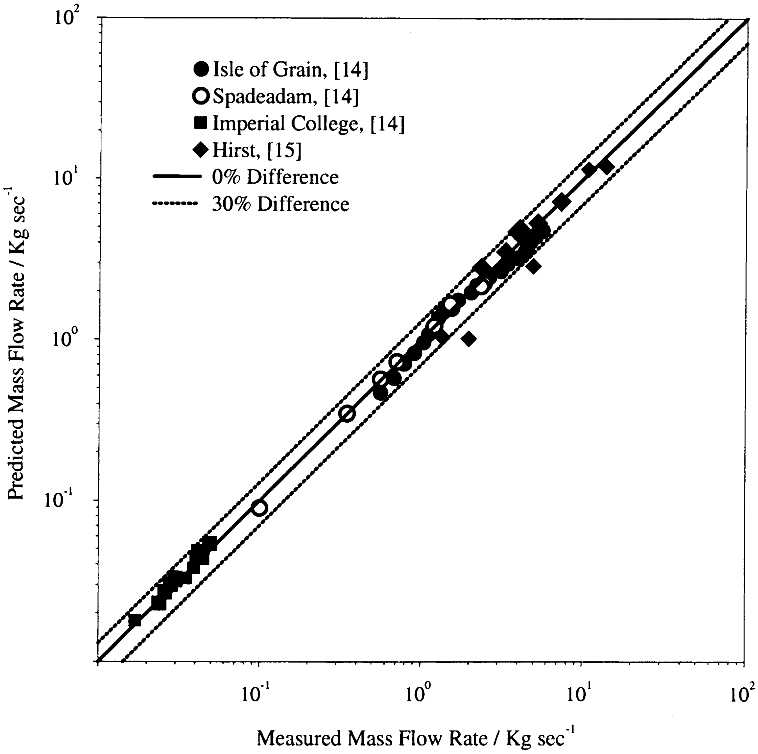

Fig. 4. Validation of the homogeneous equilibrium two-phase vent model for hydrocarbon systems.

vents tended to under predict the measured mass flow rate. This issue is ongoing and further research is required to understand why the homogeneous equilibrium model works so well for hydrocarbons flowing through short vents.

When considering top venting of a high pressure two-phase vessel, the first concern is whether two-phase venting occurs or not. Fig. 5 shows the transition from two-phase to gas phase venting for a vessel filled with refrigerant R12 at a pressure of 10 bar. The *x*-axis is the vent area relative to the cross-sectional area of the vessel and the *y*-axis is the initial liquid fill level expressed as a percentage of the total vessel volume. The measurements are taken from Wehmeir et al. [11]. An open circle in the figure indicates gas phase outflow and a full circle indicates two-phase outflow during the early stages of vessel depressurisation. Three predictions of the outflow phase transition boundary are shown in the figure. One of the curves is calculated using the criteria derived by Wehmeir et al. [11], based on a comparison of the bubble rise velocity and the velocity of the liquid–gas interface. This gives an equation for the two-phase vapour venting transition line of the form:

$$\nu_{\mathrm{f}} = \frac{\dot{m}_{\mathrm{vent,G}}}{2A_{\mathrm{vent}}U_{\mathrm{bub}}C_0\Omega + C_0\dot{m}_{\mathrm{vent,G}}}$$

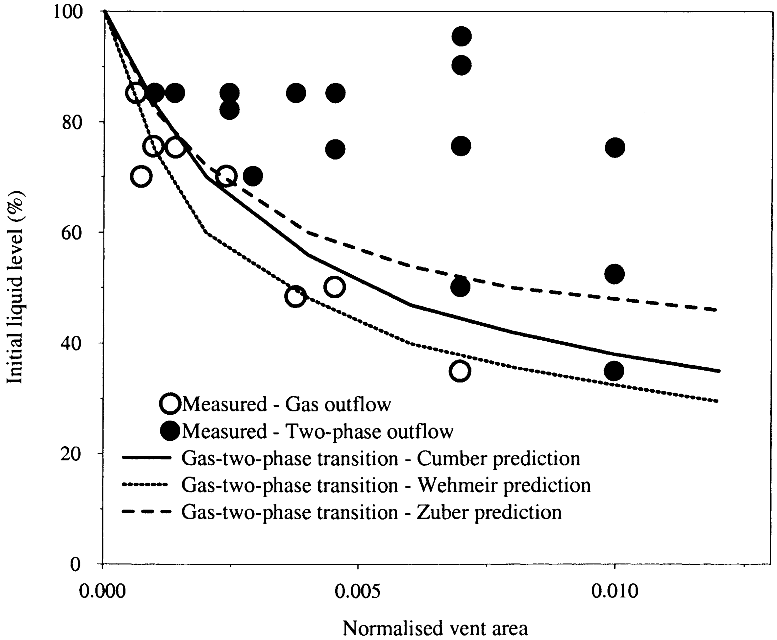

Fig. 5. Outflow from a vessel venting refrigerant R12 and the predicted two-phase vapour transition boundary.

where the radial distribution parameter is given by Kataoka and Ishii's correlation (7) and the bubble rise velocity is given by Eq. (1). The second phase transition line in Fig. 5 is calculated with the radial distribution parameter set to 1.5 and the bubble rise velocity given by Eq. (2). Zuber and Findlay [17], proposed the bubble rise correlation (2) and a value of 1.5 for the radial distribution parameter was proposed by Grolmes [18]. This combination of bubble rise velocity correlation and radial distribution parameter was used in Skouloudis's benchmarking studies of the SAFIRE model [2]. The final curve in Fig. 5 is calculated using the radial distribution parameter given by the correlation (9) and Eq. (1) for the bubble rise velocity, the equations used in the model proposed in this paper. For convenience the three lines are labelled using the first name of the references cited, as the Wehmeir, Zuber and Cumber curve, respectively. The Wehmeir curve tends to be conservative with respect to predicting the onset of two-phase venting. The model was formulated with this property as its application is vent sizing. The Zuber curve is not conservative, particularly for large vent areas. For example it predicts gas phase outflow for an initial fill level of 43% for a relative vent area of 0.01, whereas an experiment with an initial fill level of 37% gave two-phase venting. The Cumber curve is the most accurate of the three curves, correctly separating the experimental data into gas outflow and two-phase outflow except for two data points.

A typical experiment used in the calibration of the radial distribution parameter for vessels, is a saturated water vessel depressurisation [2]. The vessel volume was 50 l, filled with saturated water at an initial pressure of 2.5 bar and a void fraction of 0.02. The vent was a 20 mm diameter pipe of length 1.8 m. Fig. 6 shows the measured and predicted vessel

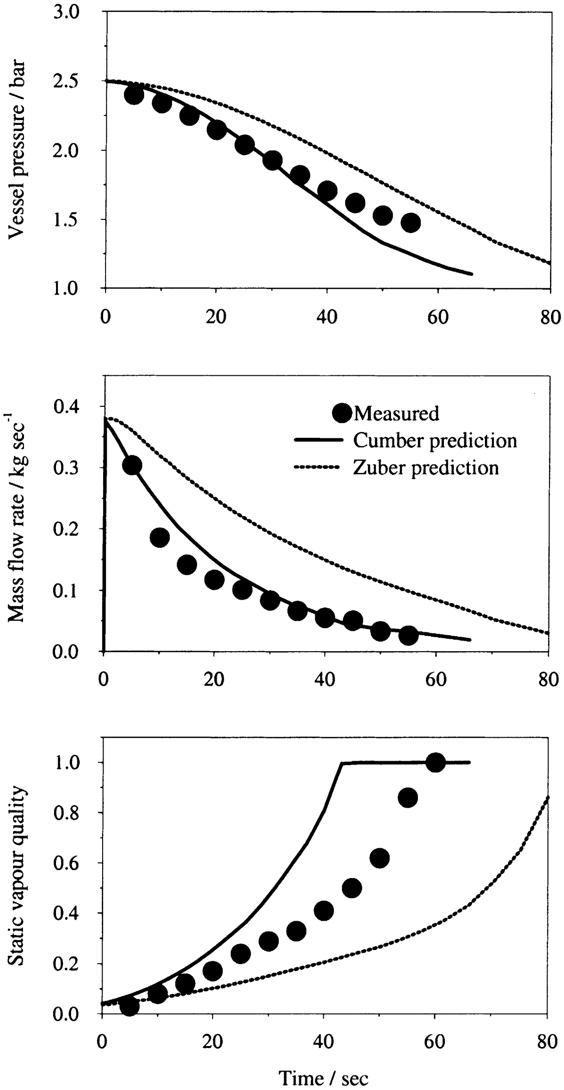

Fig. 6. Transient release of saturated water.

pressure; mass flow rate and the static exit quality. For each flow quantity two predictions are shown. The full line is a prediction calculated by the model described in this paper, for convenience labelled as the Cumber model. The dotted line is a prediction calculated using the bubble rise velocity (2) and a value of 1.5 for the radial distribution parameter, for convenience labelled as the Zuber model. The Cumber model predictions are in closer agreement with the measured flow parameters than the Zuber model. The Cumber model prediction of the final void fraction in the vessel is 0.2 compared to a measured value of 0.22

and the Zuber model prediction of 0.33. This is encouraging but not altogether compelling evidence of the accuracy of the Cumber model as this experiment was used in the calibration of the radial distribution parameter for closed systems.

The final two experiments used to evaluate the proposed vessel depressurisation model are interesting because they have not been used in the model calibration and are a good test of the model's accuracy given the scarcity of experimental data. Fig. 7 shows the measured and predicted vessel pressure, mass flow rate and static exit quality for a vessel filled with

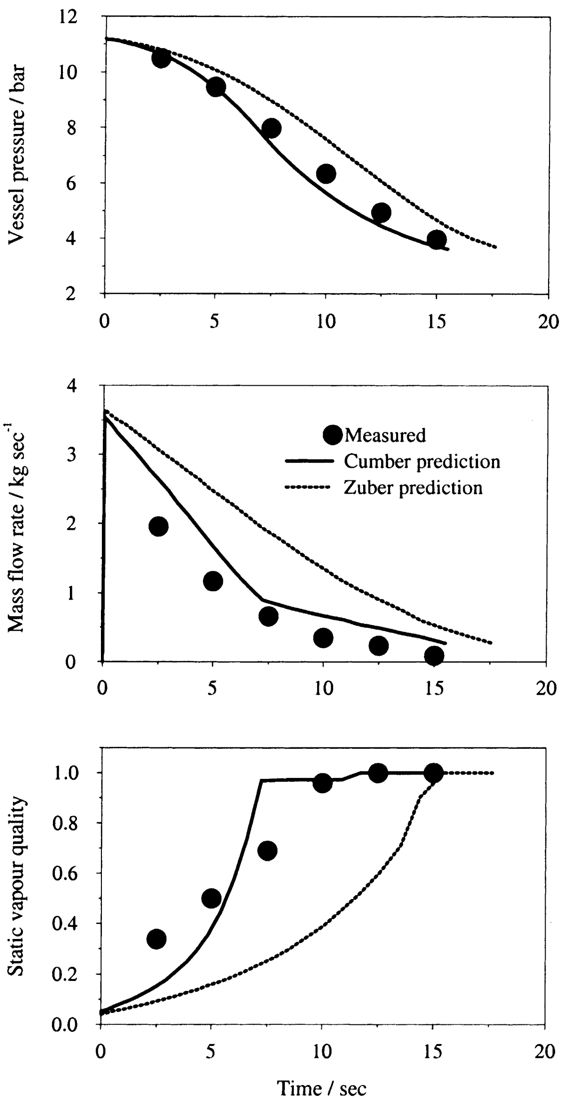

Fig. 7. Transient release of methanol.

saturated methanol at an initial pressure of 11.2 bar, and an initial fill level of 95%. The vent was an orifice with a diameter of 30 mm [19]. In this experiment the vessel had a volume of 105 l and discharged into a catch tank. When predicting the vessel depressurisation, the catch tank was modelled by adjusting the backpressure in the vessel depressurisation model to be the same as the measured pressure in the catch tank. The level of agreement between the Cumber model predictions and the measurements is similar to the saturated water vessel depressurisation experiment considered earlier. The Cumber model prediction of mass flow rate over predicts the measured mass flow rate although it is in much closer agreement than the Zuber model prediction.

The final experiment used to assess the Cumber model is a vessel filled with freon, with an initial pressure of 7 bar and an initial fill level of 85% [2]. The vent line was a pipe with a diameter of 19 mm and a length of 1.5, 0.7 m from the exit of the vessel an orifice plate with a diameter of 15 mm was located. In the simulations of the experiment, the vent is modelled as a 15 mm orifice. This simplification would tend to overestimate the mass flow rate, as the frictional losses of the pipe are not included, although this would have a second order effect on the mass flow rate as the orifice area was approximately 60% of the pipe cross-sectional area. Fig. 8 shows the measured and predicted vessel pressure; mass flow rate, static exit quality and vessel void fraction. The predictions calculated by the Cumber model and the Zuber model are similar with the Cumber model being marginally closer to the measured mass flow rate and static exit quality. The vessel pressure and the static exit quality are well predicted yet both models over predict the mass flow rate. The predicted vessel void

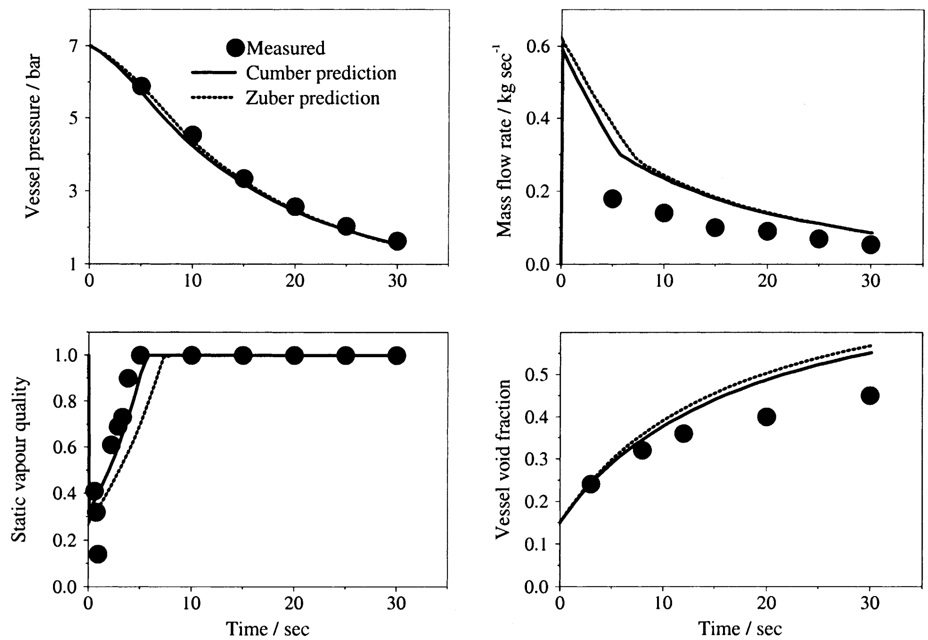

Fig. 8. Transient release of freon.

fraction of the two models are consistent with the predicted mass flow rates in that the two predictions are similar and tend to over predict the measured vessel void fraction. The Cumber model prediction of vessel void fraction is in marginally better agreement with the measurements than the Zuber model prediction. A contribution to the over prediction of the mass flow rate is the approximation of the vent line as an orifice, but it is unlikely that this is the only factor. Skouloudis [2] noted that the accurate prediction of the vessel pressure is no guarantee that other flow properties are also accurately predicted.

6. Conclusion

In this paper a mathematical model for predicting outflow for a top venting vessel undergoing level swell was described. A key aspect of the model's development was that there be no free parameters requiring adjustment by a safety engineer, with little detailed knowledge of the high-pressure system being considered. The model includes a simple extension of the radial distribution parameter for round open bubble columns to vessels. The mathematical model has been validated by comparing predicted flow parameters such as vessel pressure and mass flow rate with measurements and existing mathematical models. The new model agrees more closely with the experimental measurements than previous approaches over the range of experimental conditions considered.

Even though the new model shows good agreement with the experiments considered it should be used cautiously for conditions outside the range of the validation study. It is likely that the radial distribution parameter calibration is compensating for weaknesses in other components of the model reducing its generality. The next step in the model development would be a detailed experimental or computational study such that the bubble distribution could be calculated directly, and thereby allow a more credible calibration of the radial distribution parameter. Further work is also required to extend the model's validation, as more accurate experimental data becomes available.

References

[1] P.S. Cumber, Modelling outflow from high pressure vessels, Trans. IChemE B. Process Saf. Environ. Protect. 79 (2001) 13–22.

[2] A.N. Skouloudis, Benchmark exercises on the emergency venting of vessels, J. Loss Prevent. Process Ind. 5 (1992) 89–103.

[3] B. Boesmans, J. Berhmans, Modelling boiling delay and transient level swell during emergency pressure relief of liquefied gases, J. Hazard. Mater. 46 (1996) 93–104.

[4] H.J. Viecenz, Rise of Bubbles and Phase Separation in Vessels duing Vapour Introduction and Depressurisation, Ph.D. Thesis, University of Hanover, 1980.

[5] I. Kataoka, M. Ishii, Drift flux model for large diameter pipe and new correlation for pool void fraction, Int. J. Heat Mass Transfer 30 (1987) 1927–1939.

[6] R.C. Reid, J.M. Prausnitz, B.E. Poling, The Properties of Gases and Liquids, 4th Edition, McGraw-Hill, New York, 1987.

[7] R.M. Gibbons, A.P. Laughton, An equation of state for polar and non-polar substances and mixtures, J. Chem. Soc., Faraday Trans. 2 (80) (1984) 1019–1038.

[8] A.H. Shapiro, The Dynamics and Thermodynamics of Compressible Fluid Flow, Wiley, New York, 1953.

[9] Draft DIERS Technology Report, Emergency Relief Systems for Runaway Chemical Reactions and Storage Vessels: A Summary of Multiphase Flow Methods, Fauske and Associates, Illinois, 1984.
[10] G.B. Wallis, One Dimensional Two-Phase Flow, McGraw-Hill, New York, 1969.
[11] G. Wehmeir, F. Westphal, L. Friedel, Pressure relief system design for vapour or two-phase flow, Trans. IChemE B. Process Saf. Environ. Protect. 72 (1994) 142–148.
[12] C.M. Sheppard, Drift-flux correlation disengagement models. Part II. Shape based correlations for disengagement prediction via churn-turbulent drift–flux correlation, J. Hazard. Mater. 44 (1995) 127–139.
[13] C.M. Sheppard, S.D. Morris, Drift–flux correlation disengagement models. Part I. Theory: analytic and numeric integration details, J. Hazard. Mater. 44 (1995) 111–125.
[14] G.F. Hewit, S.M. Richardson, G. Saville, C. Weil, Two-phase Pressure Relief Sizing: An Assessment Study, Imperial College Report MPS/73, HSE, 1995.
[15] W.J.S. Hirst, Combustion of Large-Scale Jet Releases of Pressurised Liquid Propane, Institute of Gas Engineers, Communication, 1241, 1984.
[16] R. Danby, Evaluation of two-phase flow models for flashing flow in nozzles, Process Saf. Prog. AIChE 19 (2000) 32–39.
[17] N. Zuber, J. Findlay, Average volumetric concentration in two-phase flow systems, J. Heat Transfer 87 (1965) 453–463.
[18] M.A. Grolmes, A simplified approach to transient two-phase level swell, J. Multiphase Flow Heat Transfer 3 (1984) 527–538.
[19] L. Friedel, J. Schmidt, G. Wehmeier, Modelling of transient rector and catch tank, vessel pressure and mass discharge during emergency venting, in: Proceedings of the 7th International Symposium on Loss Prevention and Safety Promotion in the Process Industries, Vol. 1, 1992, pp. 1–16.